FGF1 Signaling Modulates Biliary Injury and Liver Fibrosis in the Mdr2−/− Mouse Model of Primary Sclerosing Cholangitis

April O'Brien,[1] Tianhao Zhou,[2] Tori White,[1] Abigail Medford,[1] Lixian Chen,[2] Konstantina Kyritsi,[2] Nan Wu,[2] Jonathan Childs,[1] Danaleigh Stiles,[1] Ludovica Ceci [iD],[2] Sanjukta Chakraborty [iD],[1] Burcin Ekser [iD],[3] Leonardo Baiocchi [iD],[4] Guido Carpino [iD],[5] Eugenio Gaudio [iD],[6] Chaodong Wu,[7] Lindsey Kennedy [iD],[2,8] Heather Francis [iD],[2,8] Gianfranco Alpini [iD],[2,8] and Shannon Glaser[1]

Fibroblast growth factor 1 (FGF1) belongs to a family of growth factors involved in cellular growth and division. MicroRNA 16 (miR-16) is a regulator of gene expression, which is dysregulated during liver injury and insult. However, the role of FGF1 in the progression of biliary proliferation, senescence, fibrosis, inflammation, angiogenesis, and its potential interaction with miR-16, are unknown. *In vivo* studies were performed in male bile duct–ligated (BDL, 12-week-old) mice, multidrug resistance 2 knockout (Mdr2−/−) mice (10-week-old), and their corresponding controls, treated with recombinant human FGF1 (rhFGF1), fibroblast growth factor receptor (FGFR) antagonist (AZD4547), or anti-FGF1 monoclonal antibody (mAb). *In vitro*, the human cholangiocyte cell line (H69) and human hepatic stellate cells (HSCs) were used to determine the expression of proliferation, fibrosis, angiogenesis, and inflammatory genes following rhFGF1 treatment. PSC patient and control livers were used to evaluate FGF1 and miR-16 expression. Intrahepatic bile duct mass (IBDM), along with hepatic fibrosis and inflammation, increased in BDL mice treated with rhFGF1, with a corresponding decrease in miR-16, while treatment with AZD4547 or anti-FGF1 mAb decreased hepatic fibrosis, IBDM, and inflammation in BDL and Mdr2−/− mice. *In vitro*, H69 and HSCs treated with rhFGF1 had increased expression of proliferation, fibrosis, and inflammatory markers. PSC samples also showed increased FGF1 and FGFRs with corresponding decreases in miR-16 compared with healthy controls. *Conclusion:* Our study demonstrates that suppression of FGF1 and miR-16 signaling decreases the presence of hepatic fibrosis, biliary proliferation, inflammation, senescence, and angiogenesis. Targeting the FGF1 and miR-16 axis may provide therapeutic options in treating cholangiopathies such as PSC. (*Hepatology Communications* 2022;6:1574-1588).

Cholangiocytes are the target cells in various rodent models of biliary damage, such as extrahepatic bile duct ligation (BDL) and multidrug resistance 2 knockout (Mdr2−/−, a model of primary sclerosing cholangitis [PSC]), which are associated with enhanced biliary senescence with concomitant release of senescence-associated secretory factors (SASPs, such as transforming growth factor-β1 [TGF-β1]) activating hepatic stellate cells (HSCs) by paracrine pathways.[1] PSC is a progressive liver disease characterized by inflammation, fibrosis, and narrowing of the bile ducts.

The progressive destruction of intrahepatic bile ducts eventually leads to cirrhosis and end-stage liver failure, necessitating liver transplantation, which is often the only, but not optimal, treatment option, as PSC can recur after liver transplantation.[2] During PSC pathogenesis, cholangiocytes show increased proliferation and proinflammatory signaling, which leads to an increase in hepatobiliary fibrosis, inflammatory infiltration, biliary remodeling, and cellular senescence.[3] There is growing information on the regulation of biliary damage and liver fibrosis in PSC[4]; however, there are limited and controversial data on the role of fibroblast growth factor (FGF) signaling in the modulation of PSC phenotypes.[5]

FGF1 belongs to more than 20 homologs that participate in a diverse range of functions in numerous cell types throughout the body through its interaction with one or more of the four FGF receptor subtypes (FGFR1-4).[6] FGFs can modulate various physiological functions such as cellular proliferation, migration, tissue remodeling, and DNA synthesis via receptor activation.[7] FGF1 and FGF2 regulate hepatic fibrosis[8] through the activation of HSCs, which express FGFR1-4.[9] FGF1 also plays a role in fetal hepatic development by inducing cytokeratin-19 (CK-19) expression in hepatic progenitor cells.[10]

MicroRNAs (miRs) are noncoding RNA molecules that regulate many gastrointestinal pathologies, including cancer, autoimmune disorders, and fibrotic diseases.[11] Research continues to expand on the various roles of miR-16 across multiple liver pathologies, such as the activation of HSCs.[12] Previous studies have demonstrated a potential link/feedback between FGF signaling and miR-16 in several pathologies, such as mesothelioma and angiogenic signaling in endothelial cells.[13,14] However, the role of miR-16 in the progression of PSC is undefined.

In the present study, we aimed to determine (1) the immunoreactivity/expression of FGFR1-4 and FGF1 and FGF1 serum and biliary levels in BDL and Mdr2$^{-/-}$ mice and human PSC samples; (2) the effects of recombinant human FGF1 (rhFGF1) and anti-FGF monoclonal antibody (mAb) on biliary

ARTICLE INFORMATION:

From the [1]Department of Medical Physiology, Texas A&M University College of Medicine, Bryan, TX, USA; [2]Division of Gastroenterology and Hepatology, Department of Medicine, Indiana University School of Medicine, Indianapolis, IN, USA; [3]Division of Transplant Surgery, Department of Surgery, Indiana University School of Medicine, Indianapolis, IN, USA; [4]Hepatology Unit, Dept of Medicine, University of Tor Vergata Rome, Rome, Italy; [5]Department of Movement, Human and Health Sciences, University of Rome "Foro Italico", Rome, Italy; [6]Department of Anatomical, Histological, Forensic Medicine and Orthopedics Sciences, Sapienza University of Rome, Rome, Italy; [7]Department of Nutrition, Texas A&M University, College Station, TX, USA; [8]Research, Richard L. Roudebush VA Medical Center, Indianapolis, IN, USA.

ADDRESS CORRESPONDENCE AND REPRINT REQUESTS TO:

Shannon Glaser, Ph.D.
Department of Medical Physiology, Texas A&M University
College of Medicine
MREBII – Office 2342

8447 Riverside Parkway
Bryan, TX 77807, USA
E-mail: sglaser@tamu.edu
Tel: +1-254-721-1001

damage/senescence and liver inflammation/fibrosis in BDL and Mdr2$^{-/-}$ mice; and (3) whether the effect of the FGF1/FGFR axis on liver phenotypes is associated with changes in the expression of miR-16.

Materials and Methods

MATERIALS

Immunohistochemical supplies and reagents for tissue culture were obtained from Thermo Fisher Scientific (Waltham, MA). Animals were treated with a rhFGF1 protein (GF002; MilliporeSigma, Burlington, MA), a mouse FGF acidic/FGF1 neutralizing antibody (AF4686; R&D Systems, Minneapolis, MN),[15] or a pan FGFR antagonist (AZD4547, ab216311; Abcam, Burlingame, CA).[16] Total RNA was isolated using the *mir*Vana miRNA Isolation Kit (Invitrogen, Carlsbad, CA) and reverse-transcribed with iScript Reverse Transcription Kit from Bio-Rad Laboratories (Hercules, CA). miRNA complementary DNA (cDNA) was synthesized with Taqman Advanced miRNA cDNA Synthesis Kit (A28007; Thermo Fisher Scientific). The antibodies against cytokeratin (CK-19, ab52625), desmin (ab185033), F4/80 (ab6640), FGFR1 (ab10646), FGFR2 (ab10648), FGFR3 (ab180906), FGFR4 (ab44971), cyclin-dependent kinase inhibitor 2A (p16; ab211542) as well as enzyme-linked immunosorbent assay (ELISA) kits for FGF1 (ab226587) and TGF-β1 serum analysis (ab119557) were purchased from Abcam. The FGF1 Alexa Fluor 555 conjugated antibody (bs-0229R-A555) was purchased from Bioss Antibodies (Woburn, MA). The angiogenesis antibody (SC-74528) was purchased from Santa Cruz Biotechnology (Dallas, TX). Platelet cell adhesion molecule 1 (CD31; NB-100-1642) came from Novus Biologicals (Centennial, CO). Senescence associated-β-galactosidase (SA-β-Gal) staining kit was purchased from Cell Signaling Technology (Boston, MA). Bile acid kit (MAK309-1KT) was purchased from MilliporeSigma. Primer information is listed in Supporting Table S1.

ANIMAL MODELS

All animal procedures were performed following protocols approved by the Texas A&M University

TABLE 1. EVALUATION OF LIVER TO BODY WEIGHT RATIO

	Liver Weight (g)	Body Weight (g)	Liver to Body Weight (%)
WT (n = 10)	1.35 ± 0.47	26.35 ± 4.16	5.14 ± 2.11
WT + rhFGF1 (n = 10)	1.76 ± 0.37	29.46 ± 7.43	5.71 ± 2.28
WT + AZD4547 (n = 9)	1.62 ± 0.50	26.27 ± 7.25	6.29 ± 2.65
BDL (n = 10)	1.54 ± 0.44	24.90 ± 6.96	6.26 ± 2.27
BDL + rhFGF1 (n = 10)	1.47 ± 0.14	23.81 ± 1.53	6.15 ± 0.89
BDL + AZD4547 (n = 9)	1.60 ± 0.38	24.13 ± 3.10	6.71 ± 0.26
FVB/NJ (n = 10)	1.49 ± 0.49	28.65 ± 4.86	5.19 ± 1.49
FVB/NJ + AZD4547 (n = 12)	2.01 ± 0.50	29.23 ± 2.90	6.93 ± 2.24*
FVB/NJ + anti-FGF1 mAb (n = 9)	1.54 ± 0.40	28.71 ± 2.24	5.35 ± 1.37
Mdr2$^{-/-}$ (n = 10)	3.32 ± 0.61	30.97 ± 2.84	10.76 ± 2.32*
Mdr2$^{-/-}$ + AZD4547 (n = 9)	1.59 ± 0.49	27.87 ± 3.09	5.67 ± 1.57#
Mdr2$^{-/-}$ + anti-FGF1 mAb (n = 9)	2.14 ± 0.65	29.48 ± 3.71	7.26 ± 2.78#

*P < 0.05 versus normal or WT mice.
#P < 0.05 versus Mdr2$^{-/-}$ mice.

Institutional Animal Care and Use Committee. Male C57BL/6 (25-30 g) wild-type (WT) mice and Friend virus B-type (FVB)/NJ (control for Mdr2$^{-/-}$ mice) were purchased from Jackson Laboratory (Bar Harbor, ME). Male Mdr2$^{-/-}$ mice came from in-house breeding colonies established at Texas A&M University College of Medicine, originating from mice purchased from Jackson Laboratory. All mice were housed in a temperature-controlled environment, with 12:12-hour light-dark cycles with access *ad libitum* to water and standard mouse chow. C57BL/6 mice underwent BDL as described[17] with minipump implantation occurring after ligation. Both WT and BDL mice received minipump implantation containing either rhFGF1 (100 ng/kg body weight [BW]/day) or AZD4547 (100 ng/kg BW/day)[16] (Table 1). At the age of approximately 12 weeks, male FVB/NJ and Mdr2$^{-/-}$ mice were treated with an FGFR antagonist (AZD4547; 100 ng/kg BW/day)[18] in sterile saline using an intraperitoneal Alzet osmotic minipump for 7 days, or anti-FGF1 monoclonal antibody (5 μg/100 μL saline)[15] via tail-vein injection[19] every other day

for 1 week (Table 1). Mice were euthanized either 7 days following BDL or mini-pump implantation. Animals receiving mAb treatment were euthanized 48 hours after final treatments. Liver/body weight was recorded, and serum, total liver, and cholangiocytes were collected.

ISOLATED CHOLANGIOCYTES

Virtually pure preparations of murine cholangiocytes were isolated as described[20] using immunoaffinity separation. The antibody recognizes an unidentified antigen expressed by all intrahepatic cholangiocytes (IgG_{2a}, a gift from Dr. R. A. Faris, Brown University, Providence, RI). A portion of isolated cholangiocytes were counted, resuspended, and placed in a shaking water bath for 6 hours before the supernatant was removed and stored for later use in various ELISAs.

IMMUNOREACTIVITY/ EXPRESSION OF FGFR1-4 AND FGF1 AND MEASUREMENT OF FGF1 LEVELS IN SERUM AND CHOLANGIOCYTE SUPERNATANTS

We evaluated (1) by immunofluorescence (IF) the immunoreactivity of FGFR1-4 and FGF1 in frozen liver sections (5-μm thick, six sections, four randomized animals from each treatment group) co-stained with markers of cholangiocytes (CK-19),[4] HSCs (desmin),[21] or secondary antibody only (not shown), respectively; (2) FGF1 levels in serum and cholangiocyte supernatants from selected treatment groups (n = 9) by ELISA; and (3) messenger RNA (mRNA) expression of FGFR1-4 and FGF1 (normalized to glyceraldehyde-3-phosphate dehydrogenase [GAPDH]) by quantitative polymerase chain reaction (PCR) in isolated purified cholangiocytes (3 preparations from selected groups of animals n = 3 each preparation). Images were visualized using an Olympus Fluoview FV3000 Confocal Scanning Microscope (Integrated Microscopy Imaging Laboratory, Texas A&M); quantitative PCR was performed on a QuantStudio 6 Flex Real-Time PCR System (Thermo Fisher Scientific).

MEASUREMENT OF IBDM AND BILIARY PROLIFERATION

IBDM was measured in either paraffin-embedded (WT and BDL mice) or frozen liver sections (FVB/NJ and $Mdr2^{-/-}$ mice) by immunostaining for CK-19 positive areas (5-μm thick, two slides, 10 fields per group from nine animals), which was quantified using VisioPharm software, version 2018.09 (Westminster, CO).[1] The mRNA expression of proliferation markers (proliferating cellular nuclear antigen [PCNA] and Ki67, normalized to GAPDH) was measured in isolated cholangiocytes from the selected groups of animals by quantitative PCR (three cumulative cholangiocyte preparations [n = 3 per preparation] for a total of nine animals [n = 9]).[22]

EVALUATION OF LIVER FIBROSIS AND MIR-16 EXPRESSION

Collagen deposition was evaluated by sirius red staining in paraffin-embedded liver sections (5 μm, 10 fields of view from nine animals per group) and quantified using VisioPharm software. Markers of liver fibrosis (alpha smooth muscle actin [α-SMA], collagen, type I, alpha 1 [Col1a1], and TGF-β1, normalized to GAPDH) were measured by quantitative PCR in total liver samples from the selected groups of animals (n = 9).[23] TGF-β1 serum levels were determined using a commercially available ELISA kit (Abcam). Because miR-16 is down-regulated in HSCs and contributes to the progression of liver fibrosis,[12,24] we measured, in isolated cholangiocytes, biliary miR-16 expression (normalized to U6) by quantitative PCR.[24]

MEASUREMENT OF BILIARY SENESCENCE AND LIVER INFLAMMATION AND ANGIOGENESIS

Macrophage presence was analyzed by evaluating the number of F4/80-positive cells in paraffin-embedded liver sections (5-μm thick, 10 fields from nine animals) and quantified using VisioPharm software.[25] SA-β-Gal staining was performed in frozen liver sections (10-μm thick, six fields of view from four animals) using a commercially available SA-β-Gal staining kit (Cell Signaling

Technology) following the manufacturer's protocol and quantified with VisioPharm software. We measured by quantitative PCR the mRNA expression of inflammatory (interleukin [IL]-1β and IL-6),[26] and senescence markers (cyclin dependent kinase inhibitor 1A [p21], p16, and tumor protein 53 [p53])[27] in isolated cholangiocytes from the selected groups of animals (three cumulative cholangiocyte preparations, n = 9 mice). GAPDH was used as a housekeeping gene. FGF1 stimulates decreased miR-16 expression in cholangiocytes (see "Results" section) and HSCs[12,24]; and miR-16 is predicted to regulate vascular endothelial growth factor A (VEGFA)[28] and affects liver angiogenesis by paracrine mechanisms (see Ingenuity Pathway Analysis [IPA] software; Supporting Fig. S4). Therefore, we evaluated angiogenesis by measuring the immunoreactivity of CD31 by IF in frozen liver sections (4-5-μm thick, 10 fields of view from four animals) and mRNA expression of the angiogenic factors, VEGFA, angiogenin (ANG), and CD31 (normalized to GAPDH) in either isolated cholangiocytes (ANG, VEGFA) or total liver samples (ANG, CD31) from the selected groups of animals (n = 9 mice).

IN VITRO STUDIES IN CELL LINES OF HUMAN INTRAHEPATIC BILIARY CELLS AND HUMAN HSCS

We evaluated FGFR1-4 gene expression in the immortalized normal intrahepatic cell line, human cholangiocyte cell line (H69; a gift of Dr. Gregory Gores, Mayo Medical School, Rochester, MN),[29] and HSCs[30] by reverse-transcription PCR. Human H69 and human HSCs (purchased from ScienCell Research Laboratories, Carlsbad, CA) were cultured in six-well plates with media containing 5% serum and allowed them to grow to 70%-80% confluency. Before measuring the expression of proliferation, senescence, fibrosis, and angiogenesis markers. For quantitative PCR, the six-well plates were serum-starved overnight, then H69 or HSCs were treated for 24 hours with rhFGF1 protein (10 pg/mL; Abcam).

HUMAN SAMPLES

Human liver tissue samples (optimal cutting temperature [OCT]–embedded tissue blocks) from patients with late-stage PSC (n = 4) were obtained through Dr. Burcin Ekser under a study protocol approved by the institutional review board at Indiana University School of Medicine, Indianapolis, Indiana. Tissues from healthy controls (OCT-embedded tissue blocks, n = 4) were purchased from Sekisui Xeno Tech (Kansas City, KS). Information about human samples can be found in Supporting Table S2.

The immunoreactivity of FGF1 and corresponding receptors (FGFR1-4) was evaluated by IF in liver sections (4-5-μm thick, co-stained with CK-19 or desmin, six fields of view from four samples) from healthy controls or patients with PSC. Antibodies were diluted 1:100 in 5% donkey serum, overnight at 4°C. FGF1 (ab9588), FGFR1 (ab829), FGFR2 (ab10648), and FGFR3 (ab180906) were purchased from Abcam, and FGFR4 (11098-1-AP) from Proteintech (Rosemont, IL). We also measured the expression of miR-16 by quantitative PCR in total liver samples from healthy controls and late-stage PSC samples.

STATISTICAL ANALYSIS

All data are expressed as the mean ± SEM. Differences between groups were determined using Student unpaired t test for analysis of two groups, and one-way analysis of variance when more than two groups were analyzed by the appropriate *post hoc* test. A P value of < 0.05 was deemed significant.

Results

IMMUNOREACTIVITY/EXPRESSION OF FGF RECEPTORS AND FGF1 AND FGF1 SECRETION

FGFR1-4 were evaluated by IF immunoreactivity in cryopreserved total liver OCT sections, co-stained with either desmin (a marker of activated HSCs) or CK-19 (a marker of cholangiocytes) in either BDL or Mdr2$^{-/-}$ mice and their corresponding controls (Figs. 1 and 2). There were increases in immunoreactivity in receptors 1 through 4 in the cholangiocytes, which was especially prevalent in receptor 3 of the BDL animals. HSCs had increased immunoreactivity in receptors 1, 2, and 4, and to a much
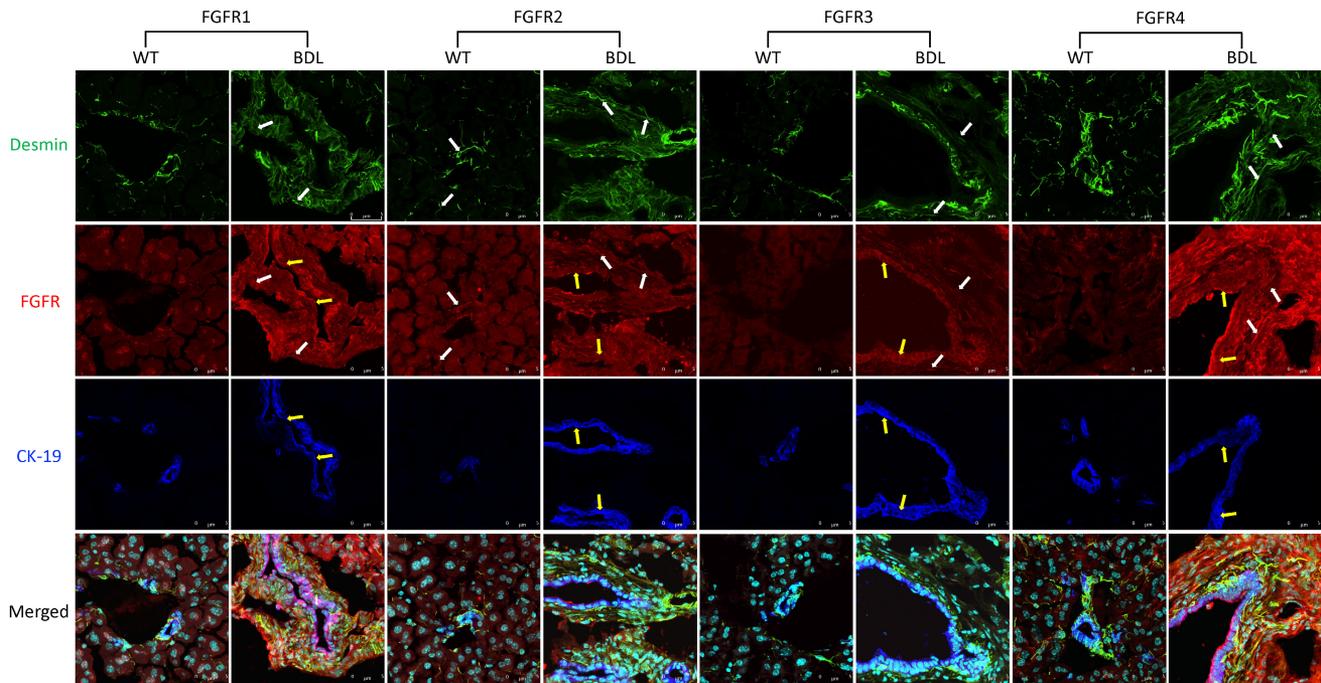
FIG. 1. By IF in liver sections there was immunoreactivity of FGFR1-4 in cholangiocytes, indicated by yellow arrows, and at lower levels in HSCs, marked with white arrows (co-stained with CK-19 or desmin, respectively) from C57BL/6 and BDL mice. Scale bar = 5 μm.

lesser extent, receptor 3 when compared with the WT control tissue. In the Mdr2$^{-/-}$ model there is a similar trend of increased CK-19 and desmin$^+$ cells when compared with the FVB control with increased immunoreactivity in both HSCs and cholangiocytes of receptor 1 (Fig. 2). Receptor 2 has no discernible immunoreactivity in the cholangiocytes in the control sample, yet there is clear staining in the HSCs. There is increased immunoreactivity in the Mdr2$^{-/-}$ sample when compared with the FVB, in both the HSCs and the cholangiocytes of FGFR2. Visually there appears to be no obvious immunoreactivity of receptor 3 in either the HSCs or cholangiocytes in the FVB control, which is only slightly increased in the Mdr2$^{-/-}$ animals. Receptor 4 immunoreactivity is increased in both cholangiocytes and HSCs in the knockout animals when compared with their FVB controls (Fig. 2). By quantitative PCR, there was enhanced mRNA expression of FGFR1-4 in cholangiocytes from BDL and Mdr2$^{-/-}$ compared with control mice (Supporting Fig. S5). We demonstrated (1) FGF1 immunoreactivity in cholangiocytes (co-stained with CK-19) in liver sections from

Mdr2$^{-/-}$ mice, and (2) increased mRNA expression of FGF1 in cholangiocytes, as well as higher FGF1 levels in serum from Mdr2$^{-/-}$ mice compared with control mice (Fig. 3A-C); no immunoreactivity for FGF1 was observed for HSCs in liver sections co-stained with desmin (Fig. 3A). The increases in FGF1 serum levels and FGF1 mRNA expression (in isolated cholangiocytes) observed in Mdr2$^{-/-}$ mice were reduced in Mdr2$^{-/-}$ mice treated with AZD4547; no changes in these parameters were observed in FVB/NJ mice treated with AZD4547 (Fig. 3A-C).

CHANGES IN IBDM AND BILIARY PROLIFERATION

In agreement with previous studies,[1,17] there was enhanced IBDM in BDL compared with WT mice (Fig. 4A), and there was increased IBDM in both WT and BDL mice treated with rhFGF1 compared with control animals, which was significantly reduced by treatment of BDL mice with AZD4547 (Fig. 4A). IBDM was significantly higher in Mdr2$^{-/-}$ compared
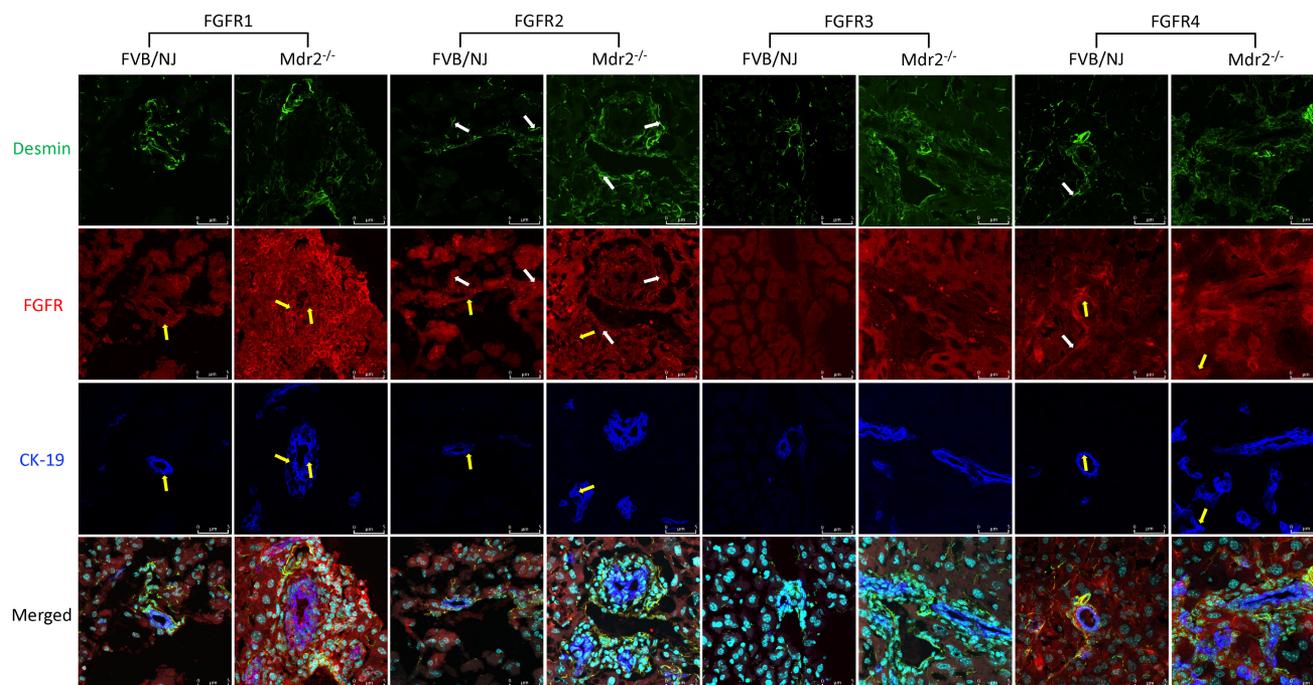
FIG. 2. By IF in liver sections there was immunoreactivity of FGFR1-4 in cholangiocytes, indicated by yellow arrows, and at lower levels in HSCs, marked with white arrows (co-stained with CK-19 or desmin, respectively) in both FVB/NJ and Mdr2$^{-/-}$ mice. Scale bar = 5 µm.

with FVB/NJ mice, which was reduced in Mdr2$^{-/-}$ mice treated with AZD4547 or anti-FGF1 monoclonal antibody, respectively (Fig. 4B). Treatment of both FVB/NJ and Mdr2$^{-/-}$ mice with rhFGF1 also increased IBDM (Supporting Fig. S6A). By quantitative PCR, there was increased expression of the proliferative markers, Ki67 and PCNA, in Mdr2$^{-/-}$ mice compared with controls, which was significantly decreased in the Mdr2$^{-/-}$ mice treated with AZD4547 (Fig. 4C).

EVALUATION OF LIVER FIBROSIS AND MIR-16 EXPRESSION

There was enhanced collagen deposition (by sirius red staining) in BDL compared with WT mice; enhanced collagen deposition was also observed in both WT and BDL mice treated with rhFGF1 compared with WT/BDL animals—increases that were significantly reduced by treatment with AZD4547 (Fig. 5A). In Mdr2$^{-/-}$ mice and rhFGF1-treated animals, there was enhanced liver fibrosis (by sirius red staining) compared with FVB/NJ mice, which was reduced by treatment with AZD4547 or

anti-FGF1 mAb, respectively (Fig. 5B, Supporting Fig. S6B). There was increased mRNA expression of α-SMA, Col1a1, and TGF-β1 in total liver samples and TGF-β1 serum levels in Mdr2$^{-/-}$ compared with FVB/NJ mice, which was decreased by AZD4547 or anti-FGF1 mAb compared with Mdr2$^{-/-}$ mice (Fig. 5C,D). As shown in Fig. 5E, there was (1) decreased expression of miR-16 in cholangiocytes from both BDL and Mdr2$^{-/-}$ mice compared with their corresponding control mice; (2) reduced expression of miR-16 in cholangiocytes from both WT and BDL mice treated with rhFGF1 compared to the corresponding control mice (Fig. 5E); and (3) either restoration of miR-16 expression (WT, BDL) or miR-16 expression increase (FVB, Mdr2$^{-/-}$) in animals treated with AZD4547 (Fig. 5E).

MEASUREMENT OF LIVER INFLAMMATION, BILIARY SENESCENCE, AND ANGIOGENESIS

By immunohistochemistry in liver sections, there was increased F4/80 immunoreactivity in BDL mice compared with controls, which
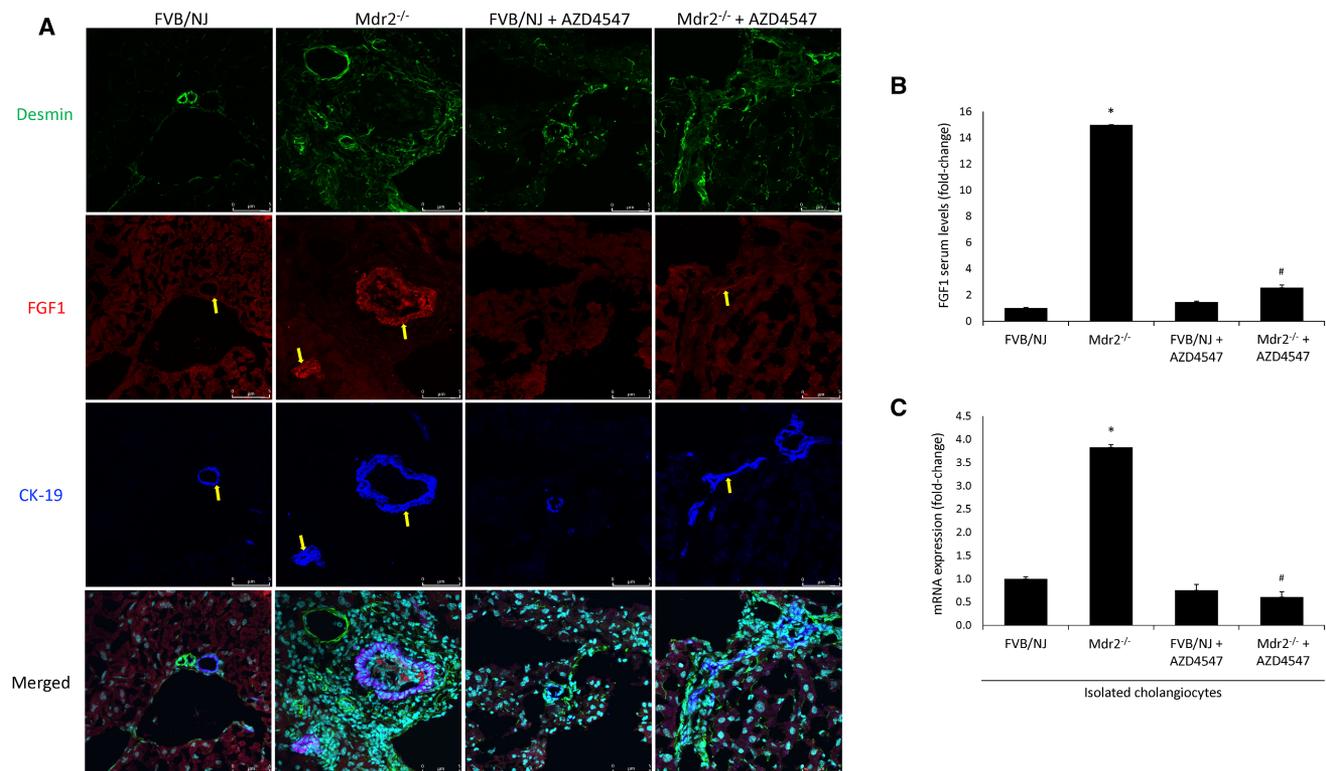
FIG. 3. (A) There was enhanced immunoreactivity for FGF1 (red) in cholangiocytes (blue) in liver sections co-stained with CK-19 from Mdr2$^{-/-}$ mice, and immunoreactivity that was decreased by treatment with AZD4547; no immunoreactivity for FGF1 was observed for HSCs in liver sections co-stained with desmin (green). Scale bar = 5 μm. (B,C) There was increased mRNA expression of FGF1 in cholangiocytes and higher FGF1 levels in serum from Mdr2$^{-/-}$ mice compared with FVB/NJ mice. Data are presented as mean ± SEM of four quantitative PCR reactions from three cumulative preparations of cholangiocytes from nine mice. Serum levels were measured in three samples from nine different animals. *$P < 0.05$ versus FVB/NJ mice; #$P < 0.05$ versus Mdr2$^{-/-}$ mice.

was ameliorated following the treatment with AZD4547 (Fig. 6A). F4/80 immunoreactivity was increased in both WT and BDL mice treated with rhFGF1 (Fig. 6A). Similarly, in Mdr2$^{-/-}$ mice there was increased F4/80 immunoreactivity compared with FVB/NJ mice, which were reduced by treatment with either AZD4547 or anti-FGF1 mAb (Fig. 6B). Like the acute injury animals, treatment with rhFGF1 increased macrophage presence in both FVB/NJ and Mdr2$^{-/-}$ animals (Supporting Fig. S6C). Furthermore, biliary mRNA expression of the SASPs, IL-6, and IL-1β (Fig. 6C), and IL-1β serum levels (Fig. 6D) were higher in Mdr2$^{-/-}$ compared with FVB/NJ mice—increases that were reduced in Mdr2$^{-/-}$ mice treated with AZD4547 (Fig. 6C,D). By SA-β-Gal staining and IF for p16 in liver sections, we observed enhanced biliary senescence in Mdr2$^{-/-}$ compared with FVB/NJ mice, which was significantly decreased in response to AZD4547 treatment (Supporting Fig. S1A,B). In addition to biliary senescence, IF for p16 also demonstrated increased immunoreactivity in desmin-positive HSCs in Mdr2$^{-/-}$ mice compared with FVB/NJ controls. Similarly, there was increased mRNA expression of the senescence markers, p21, p53 and p16, in isolated cholangiocytes, which was significantly decreased by treatment with AZD4547 (Supporting Fig. S1C). Immunoreactivity for CD31 was increased in frozen liver sections in Mdr2$^{-/-}$ when compared with FVB/NJ mice. There was also increased mRNA expression of ANG (in isolated cholangiocytes and total liver), VEGFA (in isolated cholangiocytes), and CD31 (total liver) in Mdr2$^{-/-}$ mouse—parameters that were significantly reduced by AZD4547 (Supporting Fig. S2B,C).
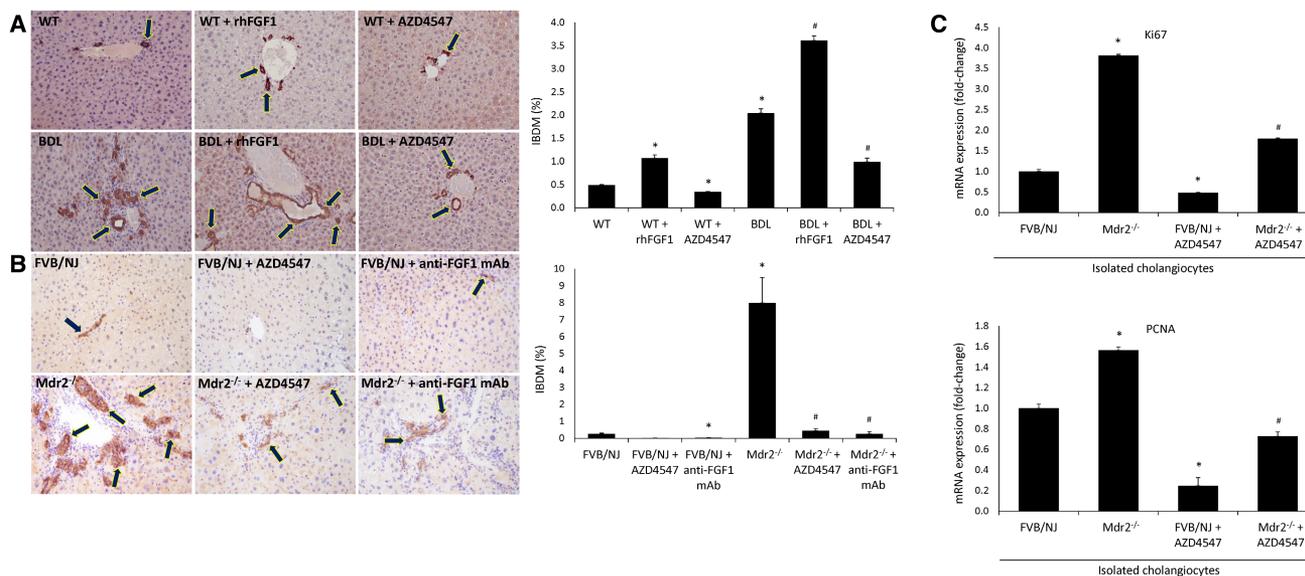
FIG. 4. (A) There was increased IBDM in BDL mice compared with C57BL/6 mice and in both C57BL/6 and BDL mice treated with recombinant human FGF1 compared with control animals—increases that were significantly reduced by AZD4547. (B) IBDM was higher in Mdr2$^{-/-}$ mice compared with FVB/NJ mice, which was reduced by AZD4547 or anti-FGF1 monoclonal antibody, respectively. Data are presented as mean ± SEM of nine total liver sections, 10 fields of view; original magnification ×20. *$P < 0.05$ versus C57BL/6 or FVB/NJ mice; #$P < 0.05$ versus BDL or Mdr2$^{-/-}$ mice. Yellow arrows indicate CK-19-positive bile ducts. (C) There was increased expression of Ki67 and PCNA in isolated cholangiocytes from Mdr2$^{-/-}$ mice compared with control that was significantly decreased in the Mdr2$^{-/-}$ mice treated with AZD4547. Data are presented as mean ± SEM of four quantitative PCR reactions from three cumulative preparations of isolated cholangiocytes from nine animals. *$P < 0.05$ versus FVB/NJ mice; #$P < 0.05$ versus Mdr2$^{-/-}$ mice.

IN VITRO STUDIES IN HUMAN H69 AND HSCS

In H69 cells treated with rhFGF1, there was enhanced mRNA expression of proliferation, fibrosis, senescence, and angiogenesis markers compared with untreated cells (Supporting Fig. S3A). In HSCs treated with rhFGF1, there was increased mRNA expression of proliferation, fibrosis, and angiogenesis markers compared with untreated cells (Supporting Fig. S3B).

FGF1 AND FGFR1-4 EXPRESSION ARE INCREASED IN PATIENTS WITH PSC

By IF in human liver sections, we observed increased immunoreactivity for FGFR1, 2, and 3 and FGF1 in bile ducts (co-stained with CK-19) in patients with PSC compared to healthy controls (Figs. 7 and 8A). There was clear colocalization with FGFR1 in both control and PSC sections, whereas FGFR2 showed cholangiocyte colocalization in PSC samples only. FGFR3 demonstrated strong immunoreactivity in the bile ducts of PSC samples, with lesser immunoreactivity in control samples (Fig. 7). Similar to FGFR3 immunoreactivity in the Mdr2$^{-/-}$ mice, FGFR4 had similar staining patterns in both controls and PSC samples, with no cholangiocyte colocalization noted. There was decreased expression of miR-16 in total liver samples from patients with PSC compared to controls (Fig. 8B).

Discussion

To further understand the molecular underpinnings of cholangiocytes pathophysiology during cholestasis, we investigated the FGF1 and miR-16 pathway in animal models of cholestasis. Our study demonstrated (1) up-regulation of FGFR1-4 in cholangiocytes
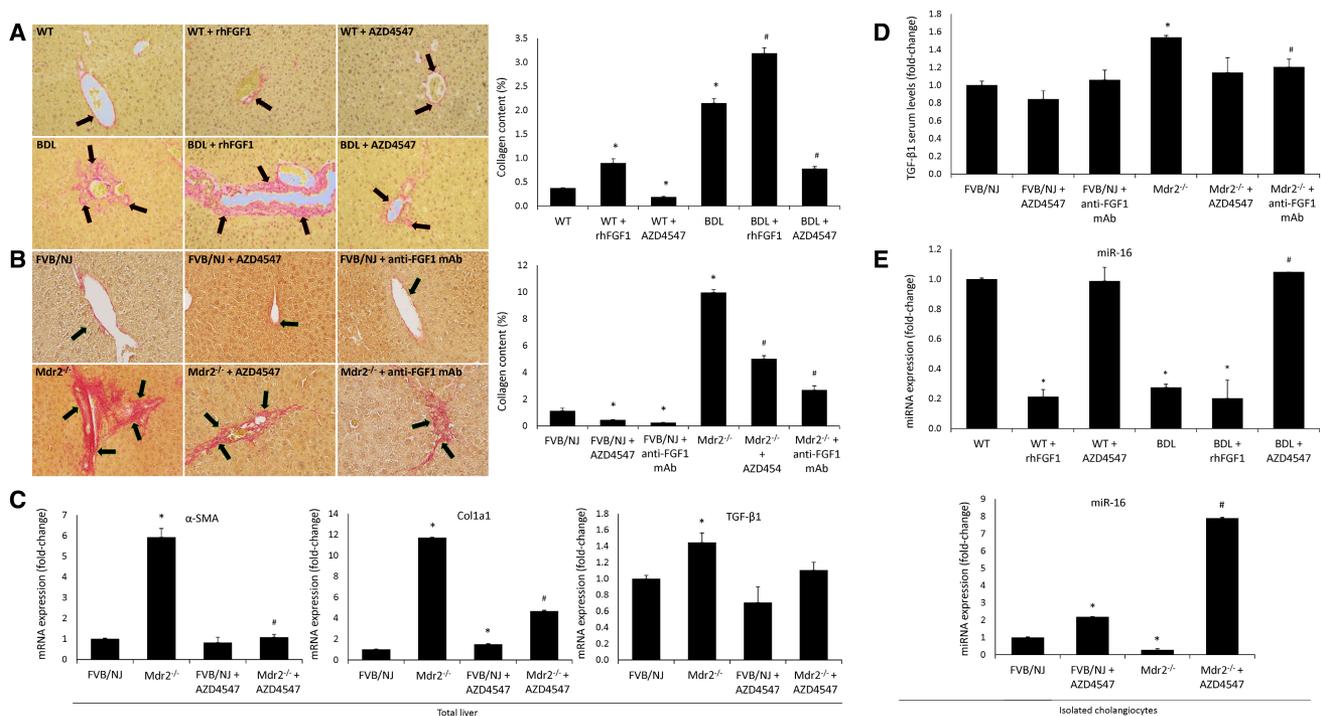
FIG. 5. (A) There was enhanced collagen deposition in BDL compared with C57BL/6 mice, as well as C57BL/6 and BDL mice treated with rhFGF1 compared with control animals—increases that were significantly reduced by treatment with AZD4547. (B) In Mdr2$^{-/-}$ mice there was enhanced liver fibrosis compared with FVB/NJ mice, which was reduced by treatment with AZD4547 or anti-FGF1 monoclonal antibody. (A,B) Data are presented as mean ± SEM of six total liver sections, 10 fields of view from nine animals; original magnification ×20. *$P < 0.05$ versus C57BL/6 or FVB/NJ mice; #$P < 0.05$ versus BDL or Mdr2$^{-/-}$ mice. Red arrows indicate collagen deposition around bile ducts. (C,D) There was increased mRNA expression of α-SMA, Col1a1, and TGF-β1 (in total liver samples) and TGF-β1 serum levels in Mdr2$^{-/-}$ mice compared with FVB/NJ mice—increases that were significantly decreased by AZD4547 or anti-FGF1 mAb compared with Mdr2$^{-/-}$ mice. Data are presented as mean ± SEM of four quantitative PCR reactions from three cumulative preparations of isolated cholangiocytes from nine animals. Data are presented as mean ± SEM of three experiments from nine animals for TGF-β1 serum levels. *$P < 0.05$ versus FVB/NJ mice; #$P < 0.05$ versus Mdr2$^{-/-}$ mice. (E) There was (1) decreased expression of miR-16 in cholangiocytes from both BDL and Mdr2$^{-/-}$ mice compared with control mice; and (2) reduced expression of miR-16 in cholangiocytes from both C57BL/6 and BDL mice treated with FGF1 compared to the corresponding control mice. Data are presented as mean ± SEM of four quantitative PCR reactions from three cumulative preparations of isolated cholangiocytes from nine animals. *$P < 0.05$ versus WT mice; #$P < 0.05$ versus BDL mice.

from BDL and Mdr2$^{-/-}$ mice; (2) cholangiocytes but not HSCs displayed immunoreactivity for FGF1; (3) administration of rhFGF1 increased ductular reaction, hepatic inflammation, and fibrosis in BDL and Mdr2$^{-/-}$ mice compared with control animals—phenotypes that were decreased following AZD4547 treatment; and (4) increased FGF1 immunoreactivity/expression and FGF levels in serum and isolated cholangiocytes as well as biliary senescence/ductular reaction, hepatic inflammation, and fibrosis in Mdr2$^{-/-}$ mice; some of these parameters were decreased in response to treatment with AZD4547 or anti-FGF1 monoclonal antibody. In late-stage human

PSC samples, there was increased immunoreactivity of FGFR1-4 and FGF1 and decreased expression of miR-16. *In vitro*, we have demonstrated that (1) H69 and HSCs express FGFR1-4; and (2) FGF1 changed the mRNA expression of proliferation, senescence, fibrosis, and angiogenesis markers in H69 and HSCs compared with basal values. These findings validate a critical role for FGF1 signaling in promoting biliary liver injury.

In support of our findings, several studies have demonstrated the role of FGF/FGFR signaling in modulating cholestatic liver diseases.[9,31-32] One study has shown that cholangiocytes express FGFR4 and
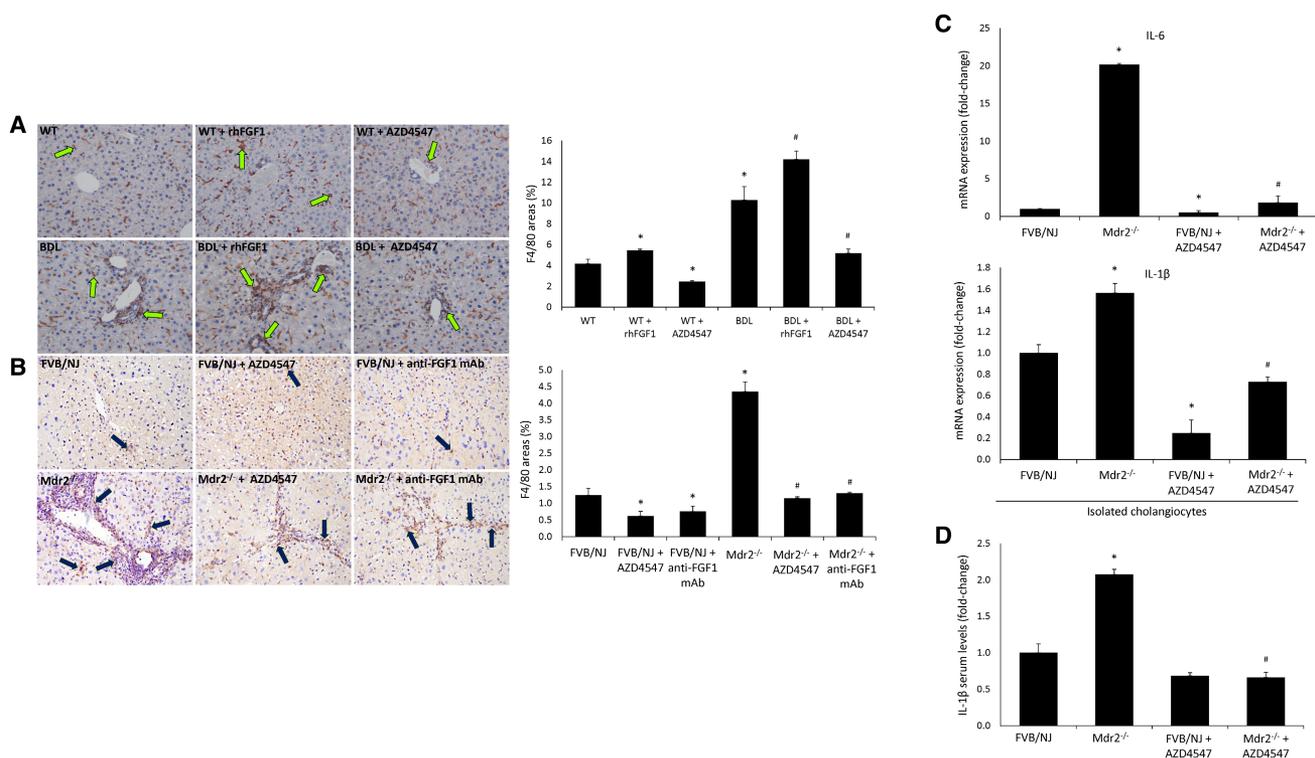
FIG. 6. (A) By immunohistochemistry in liver sections, there was increased F4/80 immunoreactivity in BDL compared with mice, which was ameliorated by treatment with AZD4547; F4/80 immunoreactivity increased in both C57BL/6 and BDL mice treated with the rhFGF1. Data are presented as mean ± SEM of six total liver sections, 10 fields of view, from nine animals; original magnification ×20. *$P < 0.05$ versus C57BL/6 mice; #$P < 0.05$ versus BDL mice. Green arrows indicate F4/80-positive cells. (B) There was increased F4/80 immunoreactivity in Mdr2$^{-/-}$ compared with FVB/NJ mice, which was reduced by treatment with either AZD4547 or anti-FGF1 mAb. Data are presented as mean ± SEM of six total liver sections, 10 fields of view, from nine animals; original magnification ×20. *$P < 0.05$ versus FVB/NJ mice; #$P < 0.05$ versus Mdr2$^{-/-}$ mice. Black arrows indicate F4/80-positive cells. (C) The mRNA expression of IL-6 and IL-1β was higher in cholangiocytes from Mdr2$^{-/-}$ compared with FVB/NJ mice, but decreased in cholangiocytes from Mdr2$^{-/-}$ mice treated with AZD4547. Data are presented as mean ± SEM of four quantitative PCR reactions from three cumulative preparations of cholangiocytes from nine animals. *$P < 0.05$ versus Mdr2$^{-/-}$ mice. (D) Mdr2$^{-/-}$ mice had increased serum IL-1β levels compared with control mice, which were decreased in Mdr2$^{-/-}$ mice treated with AZD4547 compared to vehicle-treated Mdr2$^{-/-}$ mice. Serum levels were measured in three samples from nine different animals. *$P < 0.05$ versus FVB/NJ mice; #$P < 0.05$ versus Mdr2$^{-/-}$ mice.

that farnesoid X receptor (FXR)–induced secretion of FGF15/19 inhibits CYP27 expression by a p38 kinase-dependent pathway.[31] In addition, FGFR1, 2, and 4 were shown to be up-regulated in cholangiocarcinoma (CCA) cell lines and regulate CCA growth by an autocrine mechanism.[32] Parallel to our results in BDL and Mdr2$^{-/-}$ mice, several studies have demonstrated a role for all four FGFRs in the activation of HSCs.[9] Our data showing increased FGF1 levels in serum and cholangiocyte supernatants are supported by a number of studies that have evaluated the levels of other FGF isoforms during disease states. For instance, a study has demonstrated increased

expression/serum levels of hepatic FGF19 in patients with primary biliary cholangitis (PBC) that correlates with the severity of the disease.[33] Similarly, FGF19 levels were higher in patients with cirrhotic PBC compared to healthy patients or patients with non-cirrhotic PBC.[34] Furthermore, serum FGF21 is elevated during ischemia/reperfusion-induced liver injury in patients 2 hours following liver transplantation.[35]

The FGF family is comprised of 22 FGF members, which act as critical paracrine signals in liver pathophysiology.[36] FGF1 plays a controversial and complex role in liver pathophysiology. For example, a study has shown that FGF1 ameliorates liver steatosis, fibrosis,
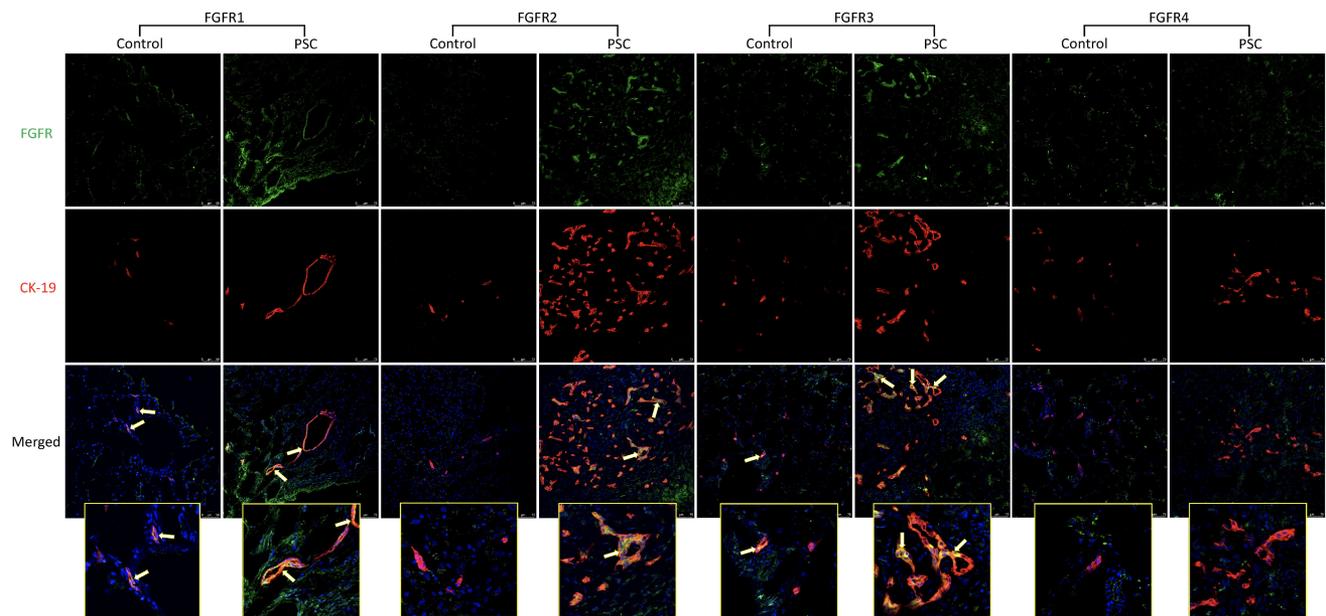
FIG. 7. There was increased FGFR1-4 immunoreactivity (co-localized with CK-19) in patients with PSC compared to healthy controls. Scale bar = 75 μm.
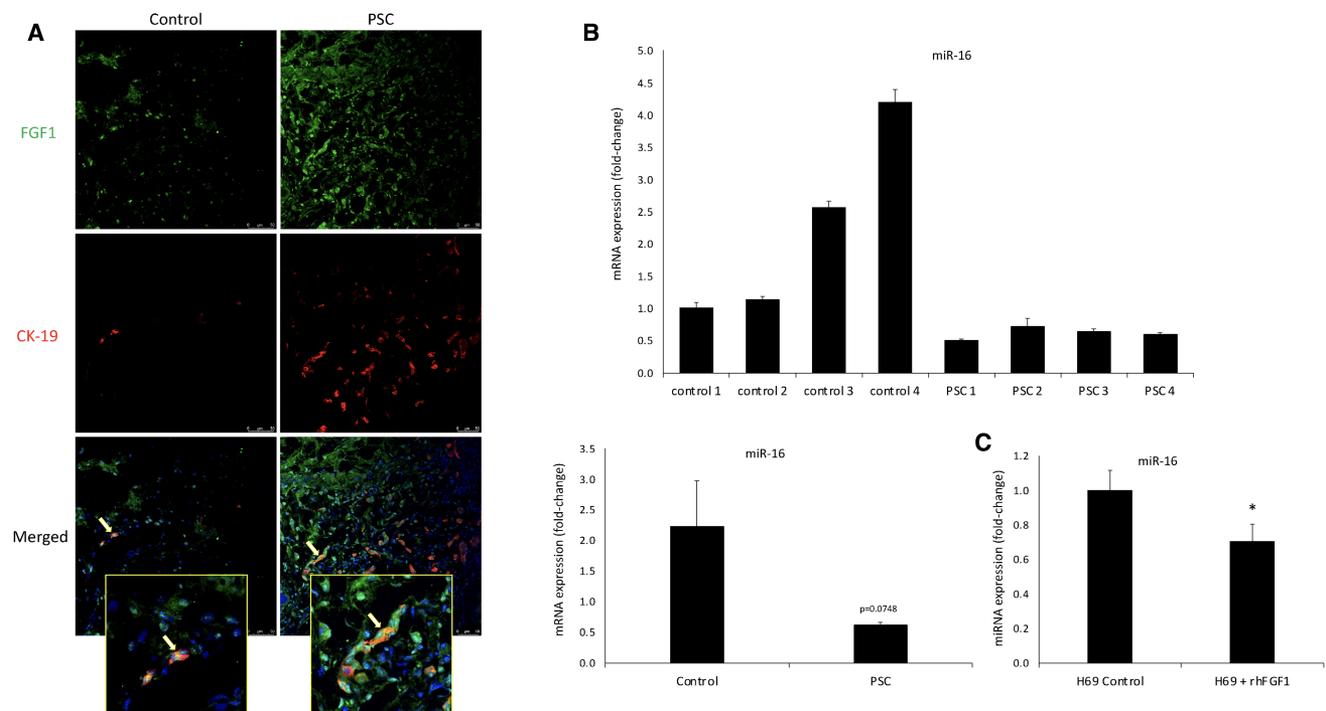
FIG. 8. (A) By IF in human liver sections, we observed increased immunoreactivity for FGF1 in bile ducts (co-stained with CK-19) in patients with PSC compared to healthy controls. Scale bar = 75 μm; secondary antibody-only samples not shown. (B) There was decreased expression of miR-16 in total liver samples from patients with PSC compared to controls, which trended toward significance. Data are presented as mean ± SEM of three experiments from serum from 4 human controls and 4 patients with PSC. * $P < 0.05$ versus controls.

and apoptosis in a diabetic mouse model of liver injury.[37] Also, FGF1 improves intrahepatic cholestasis by down-regulation of bile acid (BA) levels.[38] The beneficial effects of FGF1 and other FGF isoforms (e.g., FGF21) on steatosis and steatohepatitis were also observed in mouse models of nonalcoholic fatty liver diseases.[39] Another study has shown that elevated levels of FGF19 suppress BA synthesis through inhibition of the CYP7A1 (cytochrome P450 family 7 subfamily A member 1) gene, thus providing beneficial effects for patients with PBC.[34] Furthermore, another study demonstrated the role of FGF19 in the development of hepatocellular carcinoma in transgenic mice overexpressing FGF19 in skeletal muscle.[40] Conversely, a study by Yu et al. revealed that animals lacking in either FGF1 and/or FGF2 had significantly reduced liver fibrosis compared with controls in a carbon tetrachloride (CCl$_4$)–induced chronic injury model.[41] Also, FGF15/19 has been shown not to act as a direct profibrotic mitogen to HSCs, and the protection against fibrosis by FGF15 deficiency may be due to increased BA-dependent activation of FXR in HSCs.[9] Parallel to our findings of decreased liver fibrosis and angiogenesis with an FGFR antagonist, a recent study has shown that Brivanib (a selective inhibitor of VEGFR and FGFR tyrosine kinases) inhibits liver fibrosis and angiogenesis through the inhibition of VEGF and FGF-induced HSC proliferation in three different models of liver fibrosis including BDL.[42] Concerning the biliary epithelium, a number of studies demonstrated that stimulation of FGF/FGFR signaling not only has a role in the expansion of some forms of CCA but also contributes to the onset of pathological hallmarks, such as inflammation, cellular senescence, and fibrosis, during cholestatic, nonneoplastic injury.[43]

In our study, FGF1-induced liver fibrosis (observed in normal and cholestatic animals) may be due to enhanced biliary proliferation/ductular reaction and biliary senescence (concomitant with enhanced expression/levels of the SASP, TGF-β1), thus activating HSCs and liver fibrosis by a paracrine mechanism.[30] On the other hand, the decrease in liver fibrosis observed in cholestatic mice after treatment with an FGFR antagonist or an anti-FGF antibody is likely due to the concomitant reduction in the ductular reaction/biliary senescence and reduced release of SASPs. This tight correlation between changes in ductular reaction/biliary senescence and activation of

HSCs by a paracrine pathway is supported by our current and previous studies.[4] Supporting this concept, decreased biliary senescence signaling by down-regulation of p16 (an inhibitor of cyclin-dependent kinases) in Mdr2$^{-/-}$ mice by administration of p16 Vivo-Morpholino reduces ductular reaction and liver inflammation and fibrosis.[44] Although we have shown that FGF1 increases liver inflammation in our cholestatic mouse models, there are contrasting data regarding the role of FGF/FGFR signaling in the modulation of liver inflammation. In support of our findings, a study has shown that disruption of FGF signaling by FGFR inhibitors reduces inflammatory responses (induced by concanavalin A) in HSCs.[45]

Having demonstrated that FGF1 decreases the expression of miR-16 in cholangiocytes from both BDL and Mdr2$^{-/-}$ mice, we evaluated the expression of miR-16, which by IPA software (Supporting Fig. S4) displays close relationships with FGFR1 and angiogenesis markers such as VEGFA. Similar to the conundrum of FGF1 in hepatic injury, there are controversial data regarding the role of miR-16 in liver injury and repair. In contrast to previous studies and our findings (showing down-regulation of miR-16 in cholangiocytes in Mdr2$^{-/-}$ mice and human PSC samples), a study determined that (1) mice with acute liver failure displayed higher levels of miR-16; and (2) miR-16 knockdown reduced hepatic apoptosis and tumor necrosis factor synthesis by a B cell lymphoma 2–dependent mechanism.[46] The difference in miR-16 expression between this study and others (including our current findings)[12,24,47] may be due to the fact that their injury was acute and the mice were sacrificed within hours, likely resulting in the activation of different signaling pathways.[46] Similar to our findings, Kim et al. demonstrated down-regulation of miR-16 in both CCl$_4$-treated animals and patients with severe liver fibrosis compared to WT controls and patients with mild fibrotic phenotypes.[12] Furthermore, hepatitis B virus X protein reduces the expression of miR-16, triggering the malignant transformation of the hepatocyte line HepG2 cells *in vitro*.[47] Nonetheless, different from our experimental setting, during biliary tract malignancy, increased miR-16 levels were reported in human bile vesicles.[48] Furthermore, it has been previously established that there is a complex network of cross-talk between cholangiocytes and various hepatic residents, such as HSCs. We have shown not only a decrease in miR-16 in cholangiocytes, but

also in serum and total liver TGF-β1 from our chronic model. Previous research has shown that increases in TGF-β1 from neighboring cells activate resident HSCs, leading to and increasing the fibrotic state.[49] In this regard, the comparative evaluation, in PSC and CCA, of the FGF1/miR16 interplay may also be of interest to shed light on the possible mechanism leading from chronic biliary inflammation to cancer.

In summary, we have shown that treatment with rhFGF1 increases liver PSC phenotypes, whereas AZD4547, an FGFR antagonist, reduces cholangiocytes' proinflammatory and proliferative phenotypes and decreases biliary senescence and hepatic fibrosis in both BDL and Mdr2$^{-/-}$ mice through changes in miR-16-dependent angiogenesis. Modulation of the FGF1 and miR-16 axis may yield therapeutic targets for managing cholangiopathies such as PSC.

REFERENCES

1) Popov Y, Patsenker E, Fickert P, Trauner M, Schuppan D. Mdr2 (Abcb4) $^{-/-}$ mice spontaneously develop severe biliary fibrosis via massive dysregulation of pro- and antifibrogenic genes. J Hepatol 2005;43:1045-1054.

2) Lindström L, Jørgensen KK, Boberg KM, Castedal M, Rasmussen A, Rostved AA, et al. Risk factors and prognosis for recurrent primary sclerosing cholangitis after liver transplantation: a Nordic multicentre study. Scand J Gastroenterol 2018;53:297-304.

3) Banales JM, Huebert RC, Karlsen T, Strazzabosco M, LaRusso NF, Gores GJ. Cholangiocyte pathobiology. Nat Rev Gastroenterol Hepatol 2019;16:269-281.

4) **Wu N**, **Baiocchi L**, Zhou T, Kennedy L, Ceci L, Meng F, et al. The functional role of the secretin/secretin receptor signaling during cholestatic liver injury. Hepatology 2020;72:2219-2227.

5) Hirschfield GM, Chazouillères O, Drenth JP, Thorburn D, Harrison SA, Landis CS, et al. Effect of NGM282, an FGF19 analogue, in primary sclerosing cholangitis: a multicenter, randomized, double-blind, placebo-controlled phase II trial. J Hepatol 2019;70:483-493.

6) Sarabipour S, Hristova K. Mechanism of FGF receptor dimerization and activation. Nat Commun 2016;7:10262.

7) Li X. The FGF metabolic axis. Front Med 2019;13:511-530.

8) Li JT, Liao ZX, Ping J, Xu D, Wang H. Molecular mechanism of hepatic stellate cell activation and antifibrotic therapeutic strategies. J Gastroenterol 2008;43:419-428.

9) Schumacher JD, Kong BO, Wu J, Rizzolo D, Armstrong LE, Chow MD, et al. Direct and indirect effects of fibroblast growth factor (FGF) 15 and FGF19 on liver fibrosis development. Hepatology 2020;71:670-685.

10) Aqeilan RI, Calin GA, Croce CM. miR-15a and miR-16-1 in cancer: discovery, function and future perspectives. Cell Death Differ 2010;17:215-220.

11) Link A, Goel A. MicroRNA in gastrointestinal cancer: a step closer to reality. Adv Clin Chem 2013;62:221-268.

12) Kim KM, Han CY, Kim JY, Cho SS, Kim YS, Koo JH, et al. Gα(12) overexpression induced by miR-16 dysregulation contributes to liver fibrosis by promoting autophagy in hepatic stellate cells. J Hepatol 2018;68:493-504.

13) Schelch K, Kirschner MB, Williams M, Cheng YY, Zandwijk N, Grusch M, et al. A link between the fibroblast growth factor axis and the miR-16 family reveals potential new treatment combinations in mesothelioma. Mol Oncol 2018;12:58-73.

14) He Q, Ren X, Chen J, Li Y, Tang X, Wen X, et al. miR-16 targets fibroblast growth factor 2 to inhibit NPC cell proliferation and invasion via PI3K/AKT and MAPK signaling pathways. Oncotarget 2016;7:3047-3058.

15) Nelson AL, Dhimolea E, Reichert JM. Development trends for human monoclonal antibody therapeutics. Nat Rev Drug Discovery 2010;9:767-774.

16) Gavine PR, Mooney L, Kilgour E, Thomas AP, Al-Kadhimi K, Beck S, et al. AZD4547: an orally bioavailable, potent, and selective inhibitor of the fibroblast growth factor receptor tyrosine kinase family. Can Res 2012;72:2045.

17) Alpini G, Lenzi R, Sarkozi L, Tavoloni N. Biliary physiology in rats with bile ductular cell hyperplasia. Evidence for a secretory function of proliferated bile ductules. J Clin Invest 1988;81:569-578.

18) Schoch A, Thorey IS, Engert J, Winter G, Emrich T. Comparison of the lateral tail vein and the retro-orbital venous sinus routes of antibody administration in pharmacokinetic studies. Lab Animal 2014;43:95-99.

19) Yao TJ, Zhu JH, Peng DF, Cui Z, Zhang C, Lu PH. AZD-4547 exerts potent cytostatic and cytotoxic activities against fibroblast growth factor receptor (FGFR)-expressing colorectal cancer cells. Tumour Biol 2015;36:5641-5648.

20) Zhou T, Kyritsi K, Wu N, Francis H, Yang Z, Chen L, et al. Knockdown of vimentin reduces mesenchymal phenotype of cholangiocytes in the Mdr2$^{-/-}$ mouse model of primary sclerosing cholangitis (PSC). EBioMedicine 2019;48:130-142.

21) Kennedy L, Meadows V, Kyritsi K, Pham L, Kundu D, Kulkarni R, et al. Alemiroation of large bile duct damage by histamine-2 receptor vivo-morpholino treatment. Am J Pathol 2020;190:1018-1029.

22) Glaser S, Lam IP, Franchitto A, Gaudio E, Onori P, Chow BK, et al. Knockout of secretin receptor reduces large cholangiocyte hyperplasia in mice with extrahepatic cholestasis induced by bile duct ligation. Hepatology 2010;52:204-214.

23) Nallagangula KS, Nagaraj SK, Venkataswamy L, Chandrappa M. Liver fibrosis: a compilation on the biomarkers status and their significance during disease progression. Future Sci OA 2017;4:FSO250.

24) Guo CJ, Pan Q, Li DG, Sun H, Liu BW. miR-15b and miR-16 are implicated in activation of the rat hepatic stellate cell: an essential role for apoptosis. J Hepatol 2009;50:766-778.

25) Kinoshita M, Uchida T, Sato A, Nakashima M, Nakashima H, Shono S, et al. Characterization of two F4/80-positive Kupffer cell subsets by their function and phenotype in mice. J Hepatol 2010;53:903-910.

26) Koyama Y, Brenner DA. Liver inflammation and fibrosis. J Clin Investig 2017;127:55-64.

27) Huda N, Liu G, Hong H, Yan S, Khambu B, Yin X-M. Hepatic senescence, the good and the bad. World J Gastroenterol 2019;25:5069-5081.

28) **Qu Y**, **Liu H**, Lv X, Liu Y, Wang X, Zhang M, et al. MicroRNA-16-5p overexpression suppresses proliferation and invasion as well as triggers apoptosis by targeting VEGFA expression in breast carcinoma. Oncotarget 2017;8:72400-72410.

29) Ehrlich L, O'Brien A, Hall C, White T, Chen L, Wu N, et al. alpha7-nAChR knockout mice decreases biliary hyperplasia and liver fibrosis in cholestatic bile duct-ligated mice. Gene Expr 2018;18:197-207.

30) Wan Y, Meng F, Wu N, Zhou T, Venter J, Francis H, et al. Substance P increases liver fibrosis by differential changes in senescence of cholangiocytes and hepatic stellate cells. Hepatology 2017;66:528-541.

31) Jung D, York JP, Wang LI, Yang C, Zhang A, Francis HL, et al. FXR-induced secretion of FGF15/19 inhibits CYP27 expression in cholangiocytes through p38 kinase pathway. Pflugers Arch 2014;466:1011-1019.

32) Rizvi S, Yamada D, Hirsova P, Bronk SF, Werneburg NW, Krishnan A, et al. A hippo and fibroblast growth factor receptor autocrine pathway in cholangiocarcinoma. J Biol Chem 2016;291:8031-8047.

33) Wunsch E, Milkiewicz M, Wasik U, Trottier J, Kempińska-Podhorodecka A, Elias E, et al. Expression of hepatic fibroblast growth factor 19 is enhanced in primary biliary cirrhosis and correlates with severity of the disease. Sci Rep 2015;5:13462.

34) Li Z, Lin B, Lin G, Wu Y, Jie Y, Li X, et al. Circulating FGF19 closely correlates with bile acid synthesis and cholestasis in patients with primary biliary cirrhosis. PLoS One 2017;12:e0178580.

35) Ye D, Li H, Wang Y, Jia W, Zhou J, Fan J, et al. Circulating fibroblast growth factor 21 is a sensitive biomarker for severe ischemia/reperfusion injury in patients with liver transplantation. Sci Rep 2016;6:19776.

36) Nobuyuki I, Yoshiaki N, Morichika K. Roles of FGFs as paracrine or endocrine signals in liver development, health, and disease. Front Cell Dev Biol 2016;13:30.

37) Xu Z, Wu Y, Wang F, Li X, Wang P, Li Y, et al. Fibroblast growth factor 1 ameliorates diabetes-induced liver injury by reducing cellular stress and restoring autophagy. Front Pharmacol 2020;11:52.

38) Lin H, Zhou C, Hou Y, Li QI, Qiao G, Wang Y, et al. Paracrine fibroblast growth factor 1 functions as potent therapeutic agent for intrahepatic cholestasis by downregulating synthesis of bile acid. Front Pharmacol 2019;10:1515.

39) Bao L, Yin J, Gao W, Wang Q, Yao W, Gao X. A long-acting FGF21 alleviates hepatic steatosis and inflammation in a mouse model of non-alcoholic steatohepatitis partly through an FGF21-adiponectin-IL17A pathway. Br J Pharmacol 2018;175:3379-3393.

40) Nicholes K, Guillet S, Tomlinson E, Hillan K, Wright B, Frantz GD, et al. A mouse model of hepatocellular carcinoma: ectopic expression of fibroblast growth factor 19 in skeletal muscle of transgenic mice. Am J Pathol 2002;160:2295-2307.

41) Yu C, Wang F, Jin C, Huang X, Miller DL, Basilico C, et al. Role of fibroblast growth factor type 1 and 2 in carbon tetrachloride-induced hepatic injury and fibrogenesis. Am J Pathol 2003;163:1653-1662.

42) Nakamura I, Zakharia K, Banini BA, Mikhail DS, Kim TH, Yang JD, et al. Brivanib attenuates hepatic fibrosis in vivo and stellate cell activation in vitro by inhibition of FGF, VEGF and PDGF signaling. PLoS One 2014;9:e92273.

43) Baiocchi L, Sato K, Ekser B, Kennedy L, Francis H, Ceci L, et al. Cholangiocarcinoma: bridging the translational gap from preclinical to clinical development and implications for future therapy. Expert Opin Investig Drugs 2021;30:365-375.

44) Kyritsi K, Francis H, Zhou T, Ceci L, Wu N, Yang Z, et al. Downregulation of p16 decreases biliary damage and liver fibrosis in the Mdr2(/) mouse model of primary sclerosing cholangitis. Gene Expr 2020;20:89-103.

45) Wang C, Li Y, Li H, Zhang Y, Ying Z, Wang X, et al. Disruption of FGF signaling ameliorates inflammatory response in hepatic stellate cells. Front Cell Dev Biol 2020;8:601.

46) An F, Gong B, Wang H, Yu D, Zhao G, Lin L, et al. miR-15b and miR-16 regulate TNF mediated hepatocyte apoptosis via BCL2 in acute liver failure. Apoptosis 2012;17:702-716.

47) Wu G, Yu F, Xiao Z, Xu K, Xu J, Tang W, et al. Hepatitus B virus X protein downregulates expression of the miR-16 family in malignant hepatocytes in vitro. Br J Cancer 2011;105:146-153.

48) Li L, Masica D, Ishida M, Tomuleasa C, Umegaki S, Kalloo AN, et al. Human bile contains microRNA-laden extracellular vesicles that can be used for cholangiocarcinoma diagnosis. Hepatology 2014;60:896-907.

49) Dewidar B, Meyer C, Dooley S, Meindl-Beinker N. TGF-β in hepatic stellate cell activation and liver fibrogenesis-updated 2019. Cells 2019;8:1419.

Author names in bold designate shared co-first authorship.

Supporting Information

Additional Supporting Information may be found at onlinelibrary.wiley.com/doi/10.1002/hep4.1909/suppinfo.